Lift Guide Rail – Counterweight/Car - Suspension Systems under Seismic Excitations: the Dynamic Behaviour and Protection Measures

Stefan Kaczmarczyk

Faculty of Arts, Science and Technology, University of Northampton, UK

Keywords: Guide Rail, Counterweight/ Car, Seismic Excitation, Dynamic Response, Tuned Mass Damper

Abstract. Lift systems are susceptible to damage when buildings are subjected to strong earthquake motions. The counterweight - guide rail and car guide rail systems suffer from earthquake-induced vibrations. The most common mode of failure is the counterweight derailment. This paper reviews that dynamic phenomena and presents a model to study, to predict and to mitigate the effects of the seismic responses of guide rail – counterweight/ car – suspension systems. The application of a Tuned Mass Damper (TMD) is a convenient method to reduce the guide rail-counterweight/ car response and to control the system operating under seismic conditions. In the TMD arrangement vibrations of the counterweight/ car can be suppressed and the stresses in the guide rails reduced by the application of an auxiliary spring – damper - mass system attached to the main structure. In the counterweight system a part of the counterweight mass can be used as the auxiliary mass. The performance of the TMD can be improved by the application of an actuator force determined by a suitable feedback control algorithm.

1 INTRODUCTION

Lift installations subject to seismic conditions suffer from service disruption and damage. Various surveys have been conducted and the performance of lifts during strong earthquakes has been documented and analyzed [1-2]. For example, the statistics from the analysis of an earthquake which took place in San Fernando, California, on 9th February 1971, caused significant damage to vertical transportation systems in affected buildings, and provided a base for development of safety requirements for lifts operating in seismic risk zones [3,4]. The available statistics show that the counterweight - guide rail as well as the car guide rail systems suffer from earthquake-induced vibrations. The counterweight is the heaviest component of a lift system and the most common mode of failure is the counterweight derailment and its collision with the car. Other damage and modes of failure include bent guide rails, broken guide rail brackets, loose/ broken roller guides, moved/ damaged machine room equipment, suspension ropes/ compensating ropes damaged/ jumped out of the traction sheave/ diverter pulleys and broken/ tangled travelling cables.

A good understanding and prediction of dynamic phenomena occurring in lift installations subject to excitation forces due to earthquake ground motions is essential for developing mitigation and control strategies. The national and international safety codes [4,5] provide specific design guidance and safety measures to be applied for lift installations that operate in seismic zones. Those include the application of seismic switches / detection systems, counterweight displacement detectors, position restrainers to the car and counterweight frames, rope guards to prevent ropes jumping from the sheaves /pulleys and reinforced guide rails. Additional mitigating measures might involve damping devices and the use of a part of the counterweight as a tuned mass damper (TMD) [6]. In this paper, a dynamic model of a lift guide rail – counterweight/car - suspension system subject to seismic excitations is developed in order to analyse and assess the effectiveness of application a TMD to suppress the dynamic response of the lift system.

2 BUILDING STRUCTURE AND LIFT GUIDE RAIL – COUNTERWEIGHT/CAR - SUSPENSION SYSTEM INTERACTION MODEL

The diagram presented in Fig. 1(a) shows a typical configuration of a traction lift installation, and Fig. 1(b) illustrates a simplified model of a building (host) structure - lift guide rail – counterweight/car - suspension system subjected to seismic excitation. A mass – vertical rope system is mounted within the hoistway (well) structure. The larger (primary) mass shown on the diagram as M, represents the lift car or counteweight which is attached to the lower end of the rope (equivalent to the multi-roping arrangement in the lift suspension system) of length L and is constrained horizontally within the host structure by a spring of effective coefficient of stiffness k. This spring represents a combined flexibility of the roller guide - guide rail – guide rail bracket system. The auxiliary (secondary) mass m_d is attached to the primary mass via a spring – damper element of coefficient of stiffness k_d and coefficient of viscous damping c_d. The upper end of the rope is passing through O at the top of the well of height AB = Z_0. The system moves vertically in the hoistway at transport speed V and acceleration a. The mean quasi-static tension, mass per unit length, modulus of elasticity and cross-sectional metallic area of the rope are denoted as $T^i = \left[M + m_d + m(L-x)\right](g-a)$, m, E and A, respectively. The Eulerian spatial coordinate x is measured from the upper end downwards as shown. The lateral dynamic displacements of the rope are denoted as $v(x,t)$. They are coupled with the longitudinal displacements denoted as $u(x,t)$. The lateral and longitudinal motions of mass M are denoted as $v_M(t)$ and $u_M(t)$, respectively. The auxilliary mass m_d is constrained to move horizontally with its motion denoted as z_d. The structure is subject to ground motion $s_0(t)$ and that the structure undergoes bending deformations with displacements $v_0(t)$ at the top of the well.

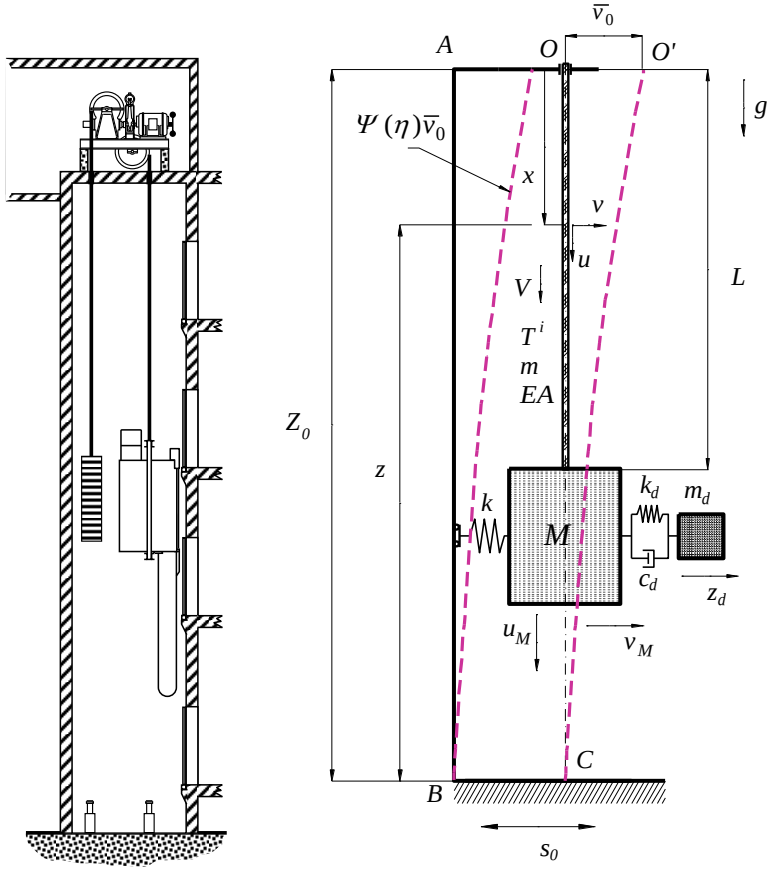

(a) (b)

Figure 1 (a) Traction lift system; (b) simplified model of the car/ counterweight mass – suspension rope system with TMD

2.1 Equations of Motion

The equations of motion can be developed by the applications of the Hamilton's principle [7] and are formulated as follows

$$\begin{aligned} &m\frac{D^2u}{Dt^2}-EA\varepsilon_x=0,\quad m\frac{D^2v}{Dt^2}-T_{ML}v_{xx}+m(g-a)(xv_{xx}+v_x)-EA(\varepsilon v_x)_x=0\\ &M\ddot{v}_M+T^l(L)v_x\big|_{x=L}+k\Delta_s-k_d(z_d-v_M)-c_d(\dot{z}_d-\dot{v}_M)+EA\,\varepsilon\big|_{x=L}v_x\big|_{x=L}=0\\ &m_d\ddot{z}_d+k_d(z_d-v_M)+c_d(\dot{z}_d-\dot{v}_M)=0,\quad (M+m_d)\ddot{u}_M+EA\,\varepsilon\big|_{x=L}=0 \end{aligned} \tag{1}$$

where $\varepsilon=u_x+v_x^2/2$ represents the axial strain, $D(\,)/Dt=(\,)_t+V(\,)_x$ $(\,)_t$ and $(\,)_x$ represent partial derivatives with respect to time t and x, respectively, $T_{ML}=(M+m_d+mL)(g-a)$ and Δ_s is the deformation of the equivalent spring k. For tensioned members such as steel wire ropes (SWR) the lateral frequencies are much lower than the longitudinal frequencies. Thus, considering that the excitations frequencies are much lower than the fundamental longitudinal frequencies the longitudinal inertia of the ropes can be neglected in the first equation in (1). This equation can be integrated to give $u_x=e(t)-v_x^2/2$ where $e(t)$ represents the quasi-static axial strain in the rope.

2.2 Resonance response to ground excitation

During the earthquake activity buildings are subject to ground (base) excitation motion. Very often the fundamental frequencies of the buildings fall within the frequency range of the ground motion [2]. Thus, in the scenario considered in this paper it is assumed that the ground motion $s_0(t)$ corresponding to the harmonic of frequency Ω_0 is exciting the fundamental mode of the building structure of the same frequency. This excitation results in bending deformations of the well structure described by the polynomial shape function $\Psi(\eta)=3\eta^2-2\eta^3$ (see Fig. 1), where $\eta=z/Z_0$ with z denoting a coordinate measured from ground level. At the top of the well ($z = Z_0$) the bending deformations lead to harmonic motions / displacements v_0 of frequency Ω_0 and of amplitude v_{0max}. In order to accommodate the base excitation in the equations of motion (1) the overall lateral displacements of the rope – mass system are expressed as

$$v(x,t)=\bar{v}(x,t)+s_0(t)+\left(1+\frac{\Psi_L-1}{L}x\right)\bar{v}_0(t),\quad \Psi_L=\Psi\left(\frac{Z_0-L}{Z_0}\right) \tag{2}$$

where $s_0(t)$ is harmonic motion of frequency Ω_0 and $\bar{v}_0(t)=v_0(t)-s_0(t)$. The relative lateral displacements $\bar{v}(x,t)$ can then be expressed using the finite series given by

$$\bar{v}(x,t)=\sum_{n=1}^{N}\Phi_n\left[x;L(\tau)\right]q_n(t) \tag{3}$$

where $q_n(t)$ represent the generalised coordinates and $\Phi_n\left[x;L(\tau)\right]$ are orthogonal trial functions depending on the spatial coordinate and the length of the ropes. In this formulation it is assumed that the lift is moving at reduced speed under the seismic conditions. Thus, the length of the rope varying slowly with time meaning that the change of L over a period corresponding to the fundamental frequency of the system is small compared to L [7]. In order to represent this fact a slow time scale defined as $\tau=\epsilon t$, where $\epsilon = 1$ is a small parameter, is introduced.

The trial functions satisfy the homogenous boundary conditions and are defined as $\Phi_n\left[x;L(\tau)\right]=\sin\left[\lambda_n(L(\tau))x\right]$, $n=1,2,\ldots,N$, with N denoting the number of terms/ modes taken in (3).

The eigenvalues $\lambda_n(L(\tau))$ that vary with the length of the rope are determined from the frequency equation given as

$$\left(k-\frac{M}{m}T_{Md}\lambda_n^2\right)\sin(\lambda_n L)+T_{Md}\lambda_n\cos(\lambda_n L)=0,\ T_{Md}\equiv T^i(L)=(M+m_d)(g-a) \tag{4}$$

It should be noted the stiffness coefficient *k* would vary with vertical motion of the mass. However, an assumption is made that this variation is small and *k* is considered to have a constant value [8]. As stated above *k* represents a combined flexibility of the roller guide and the guide rail – guide rail/ bracket system. In the analysis to follow the guide rail is modelled as multi-span beam. The coefficient of stiffness is then calculated according to BS EN81-50:2014 specifications for guide rail deflection (based on a 3-span beam model). The TMD design can then based on the worst case scenario when the system is near the resonance.

The response of the system when rth mode is subject to resonance can then be determined by considering a single-mode approximation with the relative displacements expressed as $\bar{v}(x,t)=\Phi_r[x;L(\tau)]q_r(t)$. The linearized lateral response (uncoupled from the longitudinal mode) of the main mass can then be defined by the following set of two ordinary differential equations

$$\begin{aligned}
&m_{re}\ddot{\bar{v}}_M+\tilde{c}_{re}\dot{\bar{v}}_M+\tilde{k}_{re}\bar{v}_M-k_d(z_d-\bar{v}_M)-c_d(\dot{z}_d-\dot{\bar{v}}_M)=Q_{re}(t;\tau),\\
&m_d\ddot{z}_d+k_d(z_d-\bar{v}_M)+c_d(\dot{z}_d-\dot{\bar{v}}_M)=Z_{re}(t;\tau),\\
&m_{re}=\frac{m_r}{\Phi_r^2(L)};\ \tilde{c}_{re}=\frac{\tilde{c}_r}{\Phi_r^2(L)};\ \tilde{k}_{re}=\frac{\tilde{k}_r}{\Phi_r^2(L)},\ Q_{re}(t;\tau)=\frac{Q_r(t;\tau)}{\Phi_r(L)},\ Z_{re}(t;\tau)=\frac{Z_r(t;\tau)}{\Phi_r(L)}
\end{aligned} \tag{5}$$

where modal damping is introduced through the coefficient $\tilde{c}_r=2m_r\zeta_r\tilde{\omega}_r$, where $\tilde{\omega}_r=\sqrt{\tilde{k}_r/m_r}$ and

$$\begin{aligned}
&m_r=\int_0^L\Phi_r^2dx+M\Phi_r^2(L),\ \tilde{k}_r=k_r+K_{rr},\ k_r=m_r\omega_r^2,\ \omega_r=\lambda_r\sqrt{\frac{T_{Md}}{m}},\\
&K_{rn}=m\left[g\Psi_{rn}+(g-a)(\Theta_{rn}-L\Upsilon_{rn})\right],\ \Psi_{rn}=\int_0^L x\Phi_n''\Phi_r dx,\Psi_{rn}=\int_0^L\Phi_n'\Phi_r dx,\ \Upsilon_{rn}=\int_0^L\Phi_n''\Phi_r dx,
\end{aligned} \tag{6}$$

At the right-hand sides of Eq. 5 Q_r and Z_r represent excitation functions due to the base harmonic motions.

3 COMPUTER SIMULATION TESTS AND RESULTS

The dynamic response of the system to seismic excitation is investigated through a numerical simulation of the linearized equations (5). The 4th-5th order Runge-Kutta algorithm is used in the simulation tests. The fundamental parameters of the system are presented in Table 1. In the scenario considered in the simulation the fundamental frequency of the building is given as Ω_0 = 3.3929 rad/s (0.54 Hz). The primary mass $M = P + 0.5Q$ representing a counterweight (cwt) is fitted with a TMD and travels upwards at reduced speed of 0.75 m/s. During travel the length of the ropes is changing from $L(0) = L_{max}$ = 128.66 m to to L_{min} = 8.66 m. The frequency of excitation is near the 2nd natural frequency (n = 2) and the 1st (fundamental natural frequency, n = 1) of the cwt – suspension system during the lift travel when the length of the ropes are between 120 m – 100 m and 60 m - 40 m , respectively, see Fig. 2. Fig. 3 shows the corresponding mode shapes of the system determined at L = 120 m and 45 m, respectively. The optimal value of damping ratio of the TMD system is determined as $\zeta_d=\sqrt{\frac{3\mu}{8(1+\mu)}}$, where $\mu=m_d/m_{re}$, so that $c_d=2m_d\zeta_d\omega_d$, where

$\omega_d = \sqrt{k_d / m_d}$. By noting that the ratio of natural frequencies is given as $\omega_d / \tilde{\omega}_r = (1+\mu)^{-1}$, the coefficient of stiffness of TMD is determined as $k_d = m_d \left(\frac{\tilde{\omega}_r}{1+\mu} \right)^2$.

Considering that the frequency of base excitation becomes tuned to the fundamental mode of the system when the length of the suspension ropes L is approximately 45 m the parameters of TMD are determined as m_d = 296.913 kg, k_d = 2819.9 N/m and c_d = 337.895 Ns/m. Fig. 4 and Fig. 5 show the lateral response $\bar{v}_M$ of the primary mass vs. time, and the corresponding forces acting upon the guide rail vs. time, determined by numerical simulation, with TMD action (red solid lines) and without TMD action (dashed blue lines). The plots presented in Fig. 4 correspond to the region where the frequency of excitation is near and the fundamental natural frequency and the plots in Fig. 5 correspond to the region where the frequency of excitation is near to the 2nd natural frequency of the system, respectively. Within those regions both modes are associated with the motion of cwt. It is evident that the resonance oscillations and forces are becoming attenuated by the TMD action by about 30%. In addition, Fig. 6 demonstrates that the application of TMD at the cwt results in attenuation of the rope vibrations that are associated with the 2nd mode of the system.

Table 1 Fundamental parameters of the system

Parameter	**Value**	**Unit**
Car mass P	2000	kg
Rated load mass Q	1600	kg
Rope mass per unit length m_r	0.872	kg/m
Number of ropes n_r	6	
Travel height H	120	m
Young's modulus of guide rail E_g	2.07×10^5	N/mm^2
Guide rail 2nd moment of area	947×10^4	mm^4
Guide rail bracket spacing L_g	2.5	m
Roller guide coefficient of stiffness k_{rg}	1.6674×10^5	N/m
Damping ratio ζ_r	0.25	
Fundamental frequency of the building Ω_0	0.52	Hz
Peak amplitude displacements of the building v_{0max} at $z = Z_0$	75	mm
Mass ratio μ	0.1	

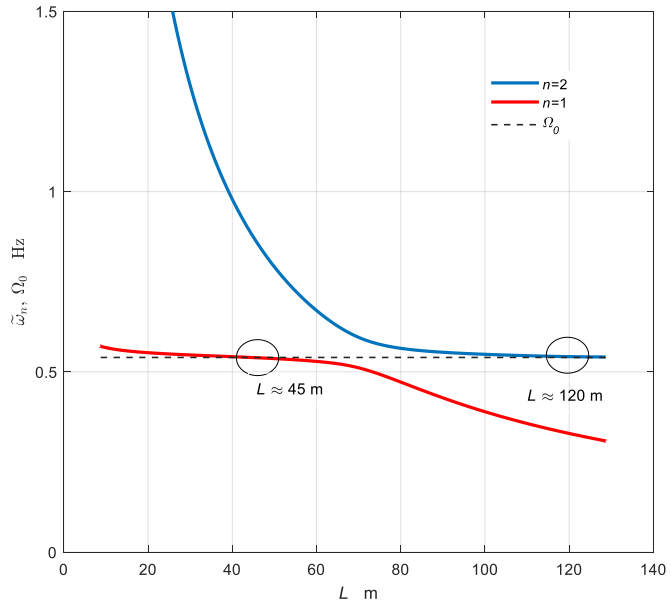

Figure 2 The 1st mode and 2nd mode natural frequencies and resonance regions.

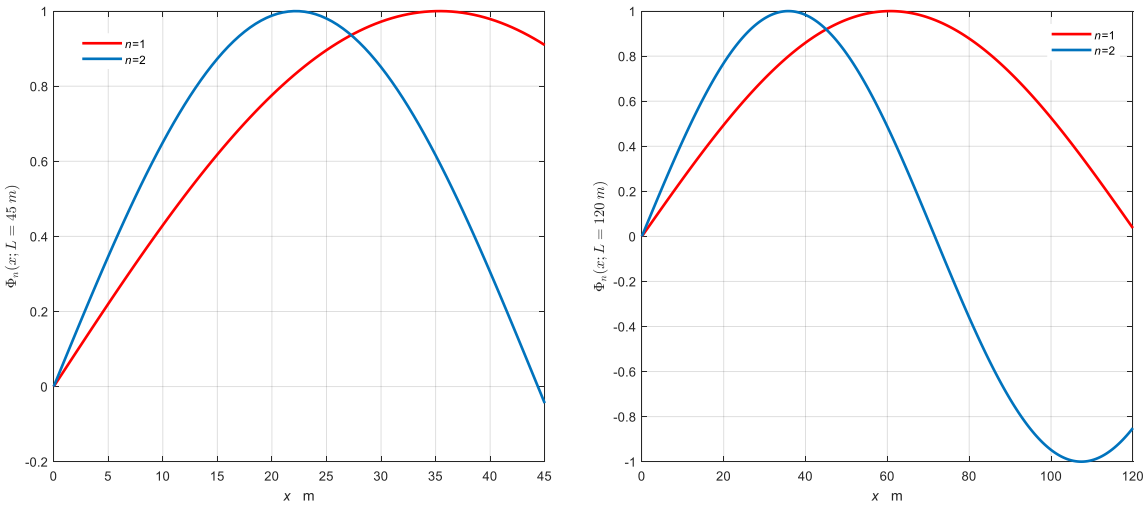

(a) **(b)**

Figure 3 The 1st mode and 2nd mode shapes (a) at *L* = 45 m, (b) at *L* = 120 m.

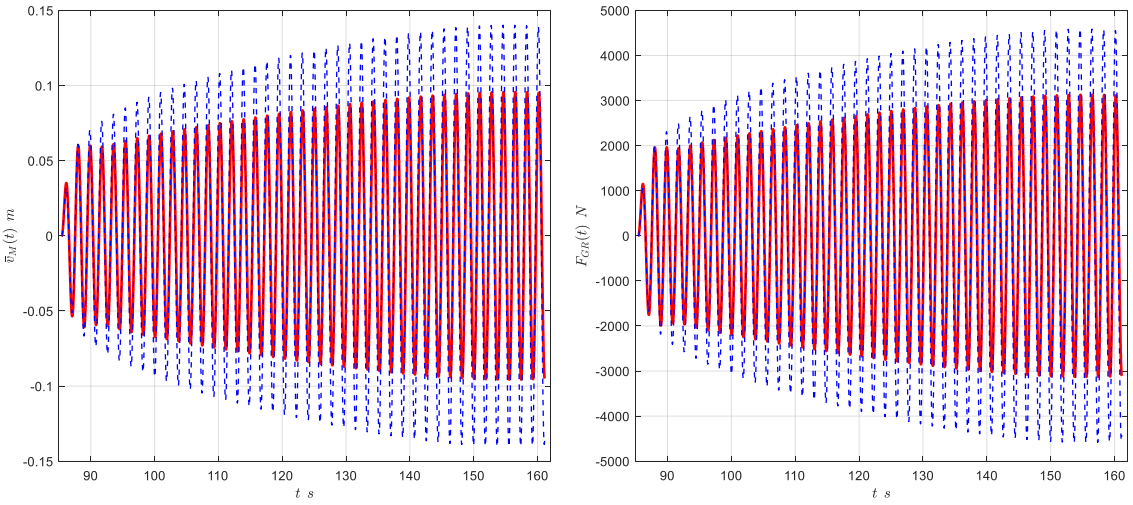

(a) **(b)**

Figure 4 (a) Displacements of the primary mass; (b) guide rail forces at the 1st mode resonance (blue dashed line without TMD and red solid line with TMD action)

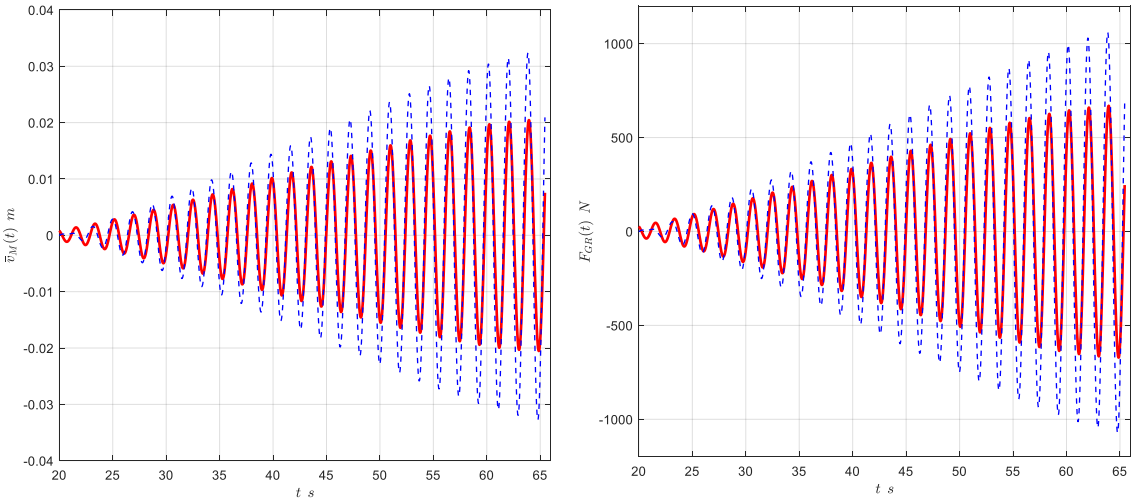

(a) (b)

Figure 5 Displacements of the primary mass (a) and guide rail forces (b) at the 2nd mode resonance (blue dashed line without TMD and red solid line with TMD action)

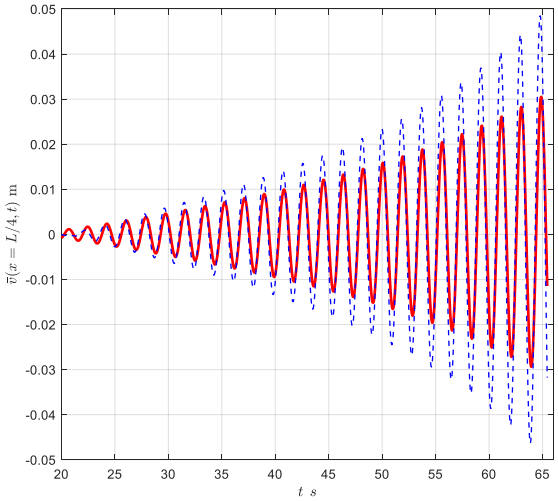

Figure 6 Displacements of the rope at *x = L/4* at the 2nd mode resonance (blue dashed line without TMD and red solid line with TMD action)

4 CONCLUDING REMARKS

Seismic-induced ground motions have adverse influence on the performance of lift installations. Dynamic models and computer simulation techniques facilitate the prediction of responses to, and mitigate the effects of, those excitations. The analysis and results presented in this paper show that under resonance conditions the application of a passive TMD system forming a part of the counterweight (or the car – frame assembly) is effective in reducing the dynamic responses and dynamic forces acting upon the lift system components. The level of reduction predicted in the case study discussed above is about 30%. In order to achieve higher performance of the system an active TMD (ATMD) can be introduced. The ATMD system is equipped with a controller, sensors and an actuator providing a control force [9].

REFERENCES

[1] L.E. Suarez, M.P. Singh, "Review of Earthquake Performance, Seismic Codes, and Dynamic Analysis of Elevators". *Earthquake Spectra*, Vol. 16, 853–878, (2000).

[2] G.C. Yao, "Seismic Performance of Passenger Elevators in Taiwan". *Earthquake Engineering and Engineering Seismology,* Vol. 3, No. 2, 17-26 (2001).

[3] E.A. Donoghue, *ASME A17.1/CSA B44 Handbook.* The American Society of Mechanical Engineers, New York (2007).

[4] The American Society of Mechanical Engineers, *Safety Code for Elevators and Escalators*. ASME A17.1-2016.

[5] British Standards Institute, *Safety rules for the construction and installation of lifts — Particular applications for passenger and good lifts. Part 77: Lifts subject to seismic conditions.* BS EN 81-77:2013.

[6] Ridlova and M.P. Singh, "Seismic protection of counterweight – rail in elevators in buildings". *Earthquake Engineering and Structural Dynamics*, Vol. 35, Issue 3, 385-394 (2006).

[7] S. Kaczmarczyk, "The Nonstationary, Nonlinear Dynamic Interactions in Slender Continua Deployed in High-rise Vertical Transportation Systems in the Modern Built Environment". *Journal of Physics: Conference Series*, Vol. 382, (2012).

[8] F. Segal, A. Rutenberg, and R. Levy, "Earthquake Response of Structure-Elevator System". *Journal of Structural Engineering,* Vol. 122, Issue 6, 607-616 (1996).

[9] S. Kaczmarczyk, S. Mirhadizadeh, "Computer Simulation Model of a Lift Car Assembly with an Active Tuned Mass Damper". *Proceedings of the 4th Symposium on Lift and Escalator Technologies*, Northampton, UK, 25-26 September 2014.